Protection from UV-induced skin carcinogenesis by genetic inhibition of the ataxia telangiectasia and Rad3-related (ATR) kinase

Masaoki Kawasumi[a,b], Bianca Lemos[a], James E. Bradner[b,c], Renee Thibodeau[a], Yong-son Kim[b], Miranda Schmidt[a], Erin Higgins[a], Sang-wahn Koo[b], Aimee Angle-Zahn[b], Adam Chen[b], Douglas Levine[b], Lynh Nguyen[a,b], Timothy P. Heffernan[b], Isabel Longo[b], Anna Mandinova[b], Yao-Ping Lu[d], Allan H. Conney[d,1], and Paul Nghiem[a,b,e,1]

[a]Division of Dermatology, Department of Medicine, University of Washington, Seattle, WA 98109; [b]Cutaneous Biology Research Center, Massachusetts General Hospital and Harvard Medical School, Charlestown, MA 02129; [c]Dana-Farber Cancer Institute, Boston, MA 02115; [d]Susan Lehman Cullman Laboratory for Cancer Research, Ernest Mario School of Pharmacy, Rutgers, The State University of New Jersey, Piscataway, NJ 08854; and [e]Clinical Research Division, Fred Hutchinson Cancer Research Center, Seattle, WA 98109

Contributed by Allan H. Conney, July 14, 2011 (sent for review April 26, 2011)

Multiple human epidemiologic studies link caffeinated (but not decaffeinated) beverage intake with significant decreases in several types of cancer, including highly prevalent UV-associated skin carcinomas. The mechanism by which caffeine protects against skin cancer is unknown. Ataxia telangiectasia and Rad3-related (ATR) is a replication checkpoint kinase activated by DNA stresses and is one of several targets of caffeine. Suppression of ATR, or its downstream target checkpoint kinase 1 (Chk1), selectively sensitizes DNA-damaged and malignant cells to apoptosis. Agents that target this pathway are currently in clinical trials. Conversely, inhibition of other DNA damage response pathways, such as ataxia telangiectasia mutated (ATM) and BRCA1, promotes cancer. To determine the effect of replication checkpoint inhibition on carcinogenesis, we generated transgenic mice with diminished ATR function in skin and crossed them into a UV-sensitive background, *Xpc*$^{-/-}$. Unlike caffeine, this genetic approach was selective and had no effect on ATM activation. These transgenic mice were viable and showed no histological abnormalities in skin. Primary keratinocytes from these mice had diminished UV-induced Chk1 phosphorylation and twofold augmentation of apoptosis after UV exposure ($P = 0.006$). With chronic UV treatment, transgenic mice remained tumor-free for significantly longer ($P = 0.003$) and had 69% fewer tumors at the end of observation of the full cohort ($P = 0.019$), compared with littermate controls with the same genetic background. This study suggests that inhibition of replication checkpoint function can suppress skin carcinogenesis and supports ATR inhibition as the relevant mechanism for the protective effect of caffeinated beverage intake in human epidemiologic studies.

skin cancer prevention | squamous cell carcinoma | xeroderma pigmentosum

Multiple human epidemiologic studies have revealed that coffee or tea intake decreases the risk of UV-associated nonmelanoma skin cancers (1–4) and non-UV–associated cancers, most prominently hepatocellular and endometrial cancers (5). In the largest study, among 93,676 women, each daily cup of caffeinated coffee consumption was dose-dependently associated with a 5% reduction in the prevalence of nonmelanoma skin cancers, whereas decaffeinated coffee had no effect, and tea had an intermediate effect, consistent with its caffeine content (3). These observations in humans hold true in multiple related studies in mice. Oral intake of caffeine in the drinking water of chronically irradiated SKH-1 hairless mice suppressed UV-induced skin cancer development (6). Topical application of caffeine in UV-pretreated "high-risk" mice also inhibited UV-induced squamous cell carcinomas (SCCs) in hairless mice by 72% (7).

UV-induced skin tumor development is a complex, long-term pathological process in vivo, and it is unclear how caffeine suppresses UV-induced tumorigenesis. Regulation of apoptosis could be one relevant factor in UV carcinogenesis, given the fact that transgenic mice expressing the apoptosis inhibitor Survivin showed accelerated development of UV-induced SCCs (8). Topical application of caffeine immediately after UV irradiation of SKH-1 hairless mice enhanced UV-induced apoptotic sunburn cells in skin (9, 10). Thus, caffeine's ability to augment elimination of UV-damaged cells via apoptosis may be relevant for its protective effects on UV-induced skin tumor development.

Caffeine is an inhibitor of several cellular processes, including activation of ataxia telangiectasia mutated (ATM) and ataxia telangiectasia and Rad3-related (ATR) (11), both of which are protein kinases that sense various types of DNA damage to block cell-cycle progression and facilitate DNA repair (12, 13). Furthermore, caffeine has other molecular targets, including cAMP phosphodiesterase, mammalian target of rapamycin (mTOR), phosphoinositide 3-kinases, and adenosine receptors (11, 14, 15). Thus, it is important to identify the molecular targets responsible for the preventive effect of caffeine in UV carcinogenesis.

Inhibition of ATR after genotoxic stress leads to premature chromatin condensation and p53-independent apoptosis (16). Thus, there is considerable interest in the pharmacologic community in targeting the replication checkpoint via ATR or its downstream target checkpoint kinase 1 (Chk1) to sensitize cancers to DNA-damaging agents (13, 17). In this study, we hypothesized that inhibition of ATR function in vivo could lead to suppression of UV-induced tumorigenesis as a potential basis for the epidemiologically significant skin cancer-preventive effects of caffeine. Conversely, there is concern that inhibition of DNA damage response pathways may lead to genomic instability and promote cancer, as is well documented for loss of ATM and BRCA1 function (18, 19). Because of these two opposing effects of DNA damage checkpoint inhibition, determination of the net effect of ATR inhibition on cancer development is best performed by in vivo experimentation.

An appealing approach to determine the net effect of suppression of ATR function is to genetically inhibit ATR in mouse skin and study susceptibility to UV carcinogenesis. The choice of an appropriate genetic system was complicated by the fact that

Author contributions: M.K., B.L., J.E.B., Y.-s.K., A.H.C., and P.N. designed research; M.K., B.L., J.E.B., R.T., Y.-s.K., M.S., E.H., S.-w.K., A.A.-Z., A.C., D.L., L.N., T.P.H., I.L., A.M., Y.-P.L., and P.N. performed research; M.K., B.L., J.E.B., R.T., M.S., E.H., Y.-P.L., A.H.C., and P.N. analyzed data; and M.K. and P.N. wrote the paper.

The authors declare no conflict of interest.

Freely available online through the PNAS open access option.

[1]To whom correspondence may be addressed. E-mail: aconney@pharmacy.rutgers.edu or pnghiem@uw.edu.

This article contains supporting information online at www.pnas.org/lookup/suppl/doi:10.1073/pnas.1111378108/-/DCSupplemental.

homozygous ATR knockout mice ($Atr^{-/-}$) were embryonic lethal (20). Heterozygous $Atr^{+/-}$ mice demonstrated a small decrease in survival and an increase in spontaneous development of tumors, including lymphoma and hepatocellular adenoma late in life (20). Mice hypomorphic for ATR (in which ATR expression was almost undetectable because of incorporation of the Seckel mutation and aberrant splicing) demonstrated no spontaneous tumor development but showed accelerated aging and diminished lifespan (21). These studies suggest that preserving significant ATR function is important for viability but that partial or tissue-specific inhibition of ATR may be well tolerated.

Here we report the generation of transgenic mice with low-level expression of a kinase-inactive form of ATR. Keratinocytes from these mice had partial inhibition of replication checkpoint function, and the mice were protected from UV-induced skin carcinogenesis. These data further support the notion that ATR inhibition is the likely mechanism for the cancer-preventive effects of caffeine.

Results

Generation of Transgenic Mice Expressing a Kinase-Inactive Form of ATR in Skin. We generated transgenic mice expressing a kinase-dead form of human ATR (ATR-kd) under the human keratin-14 (K14) promoter (Fig. 1*A*) to target expression to the basal layer of the epidermis (22). The presence of the β-globin intron (associated with improved mRNA stability) (23) was required for expression of ATR-kd under the K14 promoter, perhaps because of the large size (>8 kb) of ATR. Compared with wild-type ATR, the kinase-inactive (ATR-kd) protein has a single amino-acid substitution of Asp^{2475} to Ala in the conserved kinase domain and thus lacks kinase activity (24). ATR-kd acts as a dominant negative: previous studies showed that the phenotype of ATR-kd expression was essentially the same as that resulting from suppression of wild-type ATR function. Specifically, ATR-kd expression (24, 25), decreased ATR expression attributable to Seckel mutation (26, 27), and ATR knockdown by siRNA (28) all showed hypersensitivity to UV and decreased phosphorylation of Chk1.

Because the FVB mouse strain in which these transgenic mice were created was highly resistant to UV carcinogenesis, we crossed the ATR-kd transgenic mice into an $Xpc^{-/-}$ background. $Xpc^{-/-}$ mice have a global genome-repair deficiency, are sensitive to UV, and are prone to develop tumors after a relatively short period of UV treatment, recapitulating the human disease xeroderma pigmentosum complementation group C (XPC) (29). All ATR-kd transgenic mice and transgene-negative littermate controls used in this study were $Xpc^{-/-}$. After generating these transgenic mice, we extensively searched for phenotypic differences between ATR-kd transgenic mice and transgene-negative littermate controls. No obvious differences were noted in weight gain, macroscopic appearance of skin, density of hair, wound healing, or skin structures by histological examination. ATR-kd transgenic mice showed no spontaneous skin tumor development in either the FVB or $Xpc^{-/-}$ background.

We first confirmed stable genomic transgene integration into the transgenic mice via detection of ATR-kd DNA by using PCR (Fig. 1*B*). Next, we examined the expression of ATR-kd transgene at the RNA and protein levels. Expression of transgene mRNA was quantitated by real-time RT-PCR. Transgene mRNA was detected only in ATR-kd transgenic mice, whereas expression of a control gene (*Gapdh*) was similar in ATR-kd transgenic mice and littermate controls (Fig. 1*C*). Protein expression of FLAG-tagged ATR-kd transgene was detected after enrichment by immunoprecipitation only in transgenic mice (Fig. 1*D*). We concluded that protein expression of the FLAG-tagged transgene was low because (*i*) total ATR protein bands were similar between keratinocytes derived from transgene-negative littermate controls and from ATR-kd transgenic mice (Fig. 1*D*) and (*ii*) FLAG-tagged ATR could not be detected without immunoprecipitation (Fig. 1*D*, Input vs. IP:αFLAG).

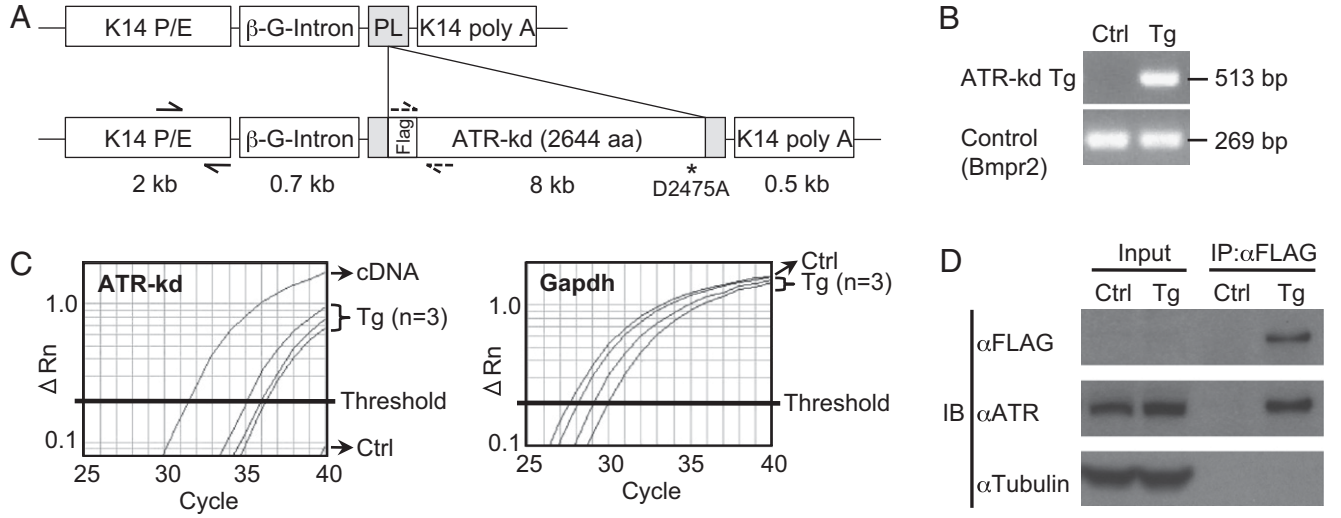

Fig. 1. Generation of K14 promoter-driven ATR-kd transgenic mice. (*A*) Schematic of ATR-kd transgene. FLAG-tagged, human ATR-kd was inserted into the polylinker (PL) region of the human K14 promoter/enhancer (P/E) construct containing a β-globin intron. Asterisk indicates the mutation site for inactivation of ATR kinase activity ($Asp^{2475} \rightarrow Ala^{2475}$). Solid arrows indicate the primer set used to detect the transgene in genomic DNA (*B*). Dashed arrows indicate the primer set used to quantify mRNA expression of the transgene (*C*). (*B*) ATR-kd transgene (ATR-kd Tg) is detected in genomic DNA from transgenic (Tg) mice, not from littermate controls (Ctrl), via PCR amplification and agarose gel analysis. (*C*) ATR-kd transgene mRNA is expressed in transgenic (Tg) mice, but not in transgene-negative littermate controls (Ctrl), as revealed by real-time RT-PCR analysis. (*Left*) Amplification plot of ATR-kd transgene. cDNA containing ATR-kd transgene sequence was used as positive control (cDNA). Samples from littermate controls (Ctrl) and negative control samples (no template) showed no amplification after 40 cycles. (*Right*) Amplification plot of the RNA quality control gene *Gapdh*. (*D*) FLAG-tagged ATR-kd protein is expressed in ATR-kd transgenic (Tg) mouse keratinocytes. Lysates (500 μg of total protein) of primary keratinocytes isolated from Tg mice and transgene-negative littermate controls (Ctrl) were used for immunoprecipitation (IP) with anti-FLAG antibody, followed by immunoblot (IB) analyses with the indicated antibodies. Input samples (15 μg of total protein) were from the same cell lysates but were not immunoprecipitated. The anti-ATR antibody used detects both human and mouse proteins.

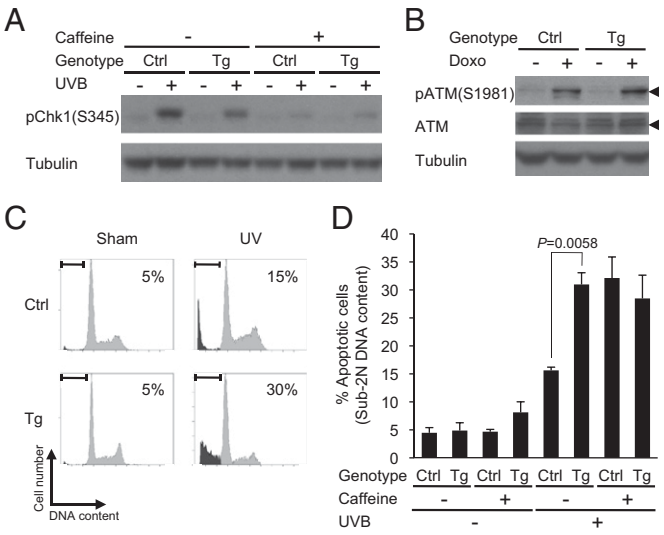

Fig. 2. Primary keratinocytes from ATR-kd transgenic mice demonstrate ATR signaling inhibition and augmentation of UV-induced apoptosis. (*A*) ATR-kd inhibits UV-induced phosphorylation of Chk1. Primary mouse keratinocytes isolated from ATR-kd transgenic (Tg) mice and transgene-negative littermate controls (Ctrl) were treated with medium or caffeine (3 mM) for 30 min before UV irradiation. Cells were irradiated with 75 mJ/cm^2 of UVB light and harvested 1 h after UV exposure for immunoblot analyses with the indicated antibodies. (*B*) ATR-kd does not inhibit doxorubicin-induced phosphorylation of ATM. Primary mouse keratinocytes isolated from ATR-kd transgenic (Tg) mice and transgene-negative littermate controls (Ctrl) were treated with medium or doxorubicin (1 μM) for 2 h and harvested for immunoblot analyses with the indicated antibodies. Arrowheads indicate same molecular size, corresponding to the ATM protein. (*C* and *D*) ATR-kd augments UV-induced apoptosis measured by sub-2N DNA content. Primary mouse keratinocytes were isolated from ATR-kd transgenic (Tg) mice and transgene-negative littermate controls (Ctrl). Cells were treated with medium or caffeine (3 mM) for 30 min before UV irradiation. Cells were irradiated with 75 mJ/cm^2 of UVB light, harvested 24 h later, and stained with propidium iodide for flow cytometry analysis. (*C*) Representative DNA content patterns of cells without caffeine treatment with percentage of sub-2N DNA content indicated. (*D*) Mean of percentage of sub-2N DNA content is shown (n = 4). (Error bars = SEM.)

ATR-kd Transgene Expression in Keratinocytes Inhibits UV Responses and Augments UV-Induced Apoptosis via ATR–Chk1 Pathway Inhibition. To investigate the effect of ATR-kd expression on UV responses in keratinocytes, we isolated primary mouse keratinocytes from ATR-kd transgenic mice and transgene-negative littermate controls. Primary keratinocytes from ATR-kd transgenic mice showed partial inhibition of UV-induced phosphorylation of Chk1, a downstream target of ATR, similar to inhibition by caffeine (nonspecific ATM/ATR inhibitor) (Fig. 2*A*).

Given the known functional similarity between ATR and ATM, we wanted to determine whether ATR-kd nonspecifically inhibits ATM activation because such nonspecificity would complicate interpretation of these studies. We assessed ATM activation via phosphorylation at Ser^{1987} in mouse ATM (which corresponds to Ser^{1981} in human ATM) (30). To avoid activating ATR, we used doxorubicin, a topoisomerase II inhibitor that selectively activates ATM compared with ATR. ATR-kd did not inhibit doxorubicin-induced phosphorylation of ATM (Fig. 2*B*). This finding demonstrates that ATR-kd selectively inhibits ATR-mediated phosphorylation, not ATM phosphorylation.

Because DNA-damaged human keratinocytes with ATR or Chk1 inhibition undergo apoptosis (28), we examined the effect of ATR-kd transgene expression on UV-induced apoptosis in keratinocytes freshly isolated from mice. Keratinocytes from transgene-positive mice showed augmentation of UV-induced apoptosis (sub-2N DNA content of 30%) compared with littermate controls (15%) (Fig. 2*C*). This augmentation by ATR-kd was similar to augmentation by caffeine in transgene-negative keratinocytes (32.1%) (Fig. 2*D*). Addition of caffeine did not further augment UV-induced apoptosis of ATR-kd keratinocytes (28.5%). These findings suggest that caffeine's ability to augment UV-induced apoptosis was mediated through ATR inhibition.

A preliminary study on apoptotic sunburn cells in epidermis was carried out in an earlier strain (FVB genetic background) of ATR-kd transgenic mice. Unlike our primary keratinocyte studies in cells derived from *Xpc*$^{-/-}$ animals, no difference between ATR-kd transgenic mice and transgene-negative littermate controls was observed in UV-induced sunburn cell formation at 6 or 10 h after 30 mJ/cm^2 of UVB light.

ATR-kd Transgenic Mice Chronically Irradiated with UV Demonstrate Longer Tumor Latency and Lower Skin Tumor Incidence. All ATR-kd transgenic mice used for chronic UV experiments were verified for transgene mRNA expression by real-time RT-PCR. The ATR-kd transgenic mouse cohort and that of transgene-negative littermate controls were carefully matched to be comparable in age, sex, and coat color between groups. All mice were verified to have *Xpc*$^{-/-}$ genotype and were irradiated with UVB light three times a week for 40 wk (cumulative UVB dosage as shown in Fig. 3*A*).

Transgene-negative littermate controls started developing tumors after 12 wk of UV treatment (Fig. 3*B*). Compared with transgene-negative littermates, ATR-kd transgene-positive mice showed significantly delayed tumor development as measured by the fraction of tumor-free mice (P = 0.0029; Fig. 3*B*) as well as a 3-wk delay in time of onset of the first tumor (P = 0.0064; Fig. 3*C*). In addition, at any given time point, the average number of tumors in ATR-kd mice was significantly lower than that in transgene-negative littermate controls (Fig. 3*D*). ATR-kd mice demonstrated 69% fewer tumors after 19 wk of UV treatment (P = 0.019).

ATR-kd Mice Demonstrate a Trend Toward Decreased Number of Invasive SCCs. Although tumor latency was extended in ATR-kd mice, continued chronic UV irradiation eventually caused tumor development in all transgene-negative littermate controls and transgenic mice by 34 wk of UV treatment. Tumors that developed in these *Xpc*$^{-/-}$ mice in the presence or absence of the ATR-kd transgene were mainly keratoacanthomas and SCCs. These lesions were similar to those previously described (29). Tumors that developed in ATR-kd mice were histologically indistinguishable from those in transgene-negative littermate controls, suggesting that ATR-kd did not affect the development of specific types of tumors and did not change the tumor spectrum.

Continued UV irradiation promotes invasive progression of tumors. We developed criteria for clinically identifying invasive SCCs in UV-irradiated mice to monitor tumor progression by visual inspection without biopsy (which would eliminate developing tumors). The criteria were based on three visible tumor features: (*i*) ≥3-mm tumor diameter; (*ii*) bleeding from a tumor; and (*iii*) ulceration, cratering, or erosion of a tumor. The clinical definition of invasive SCC required that a tumor be ≥3 mm and also display bleeding, ulceration/cratering/erosion, or both. Histological analyses of tumors on UV-irradiated mice revealed that these clinical criteria for invasive SCC strongly correlated with histological diagnosis (Fig. 3*E*). Tumors without bleeding or ulceration/cratering/erosion were in situ tumors in 13 of 14 specimens, regardless of tumor diameter. All tumors that met the clinical criteria for invasive SCCs were in fact histologically invasive SCCs (33 of 33 tumors).

Using these validated visual criteria for invasive SCC, we monitored the emergence of these tumors during chronic UV treatment. We found that ATR-kd mice developed four times fewer invasive SCCs than transgene-negative littermate controls did (0.08 vs. 0.33 invasive SCCs per mouse; Fig. 3*F*), although

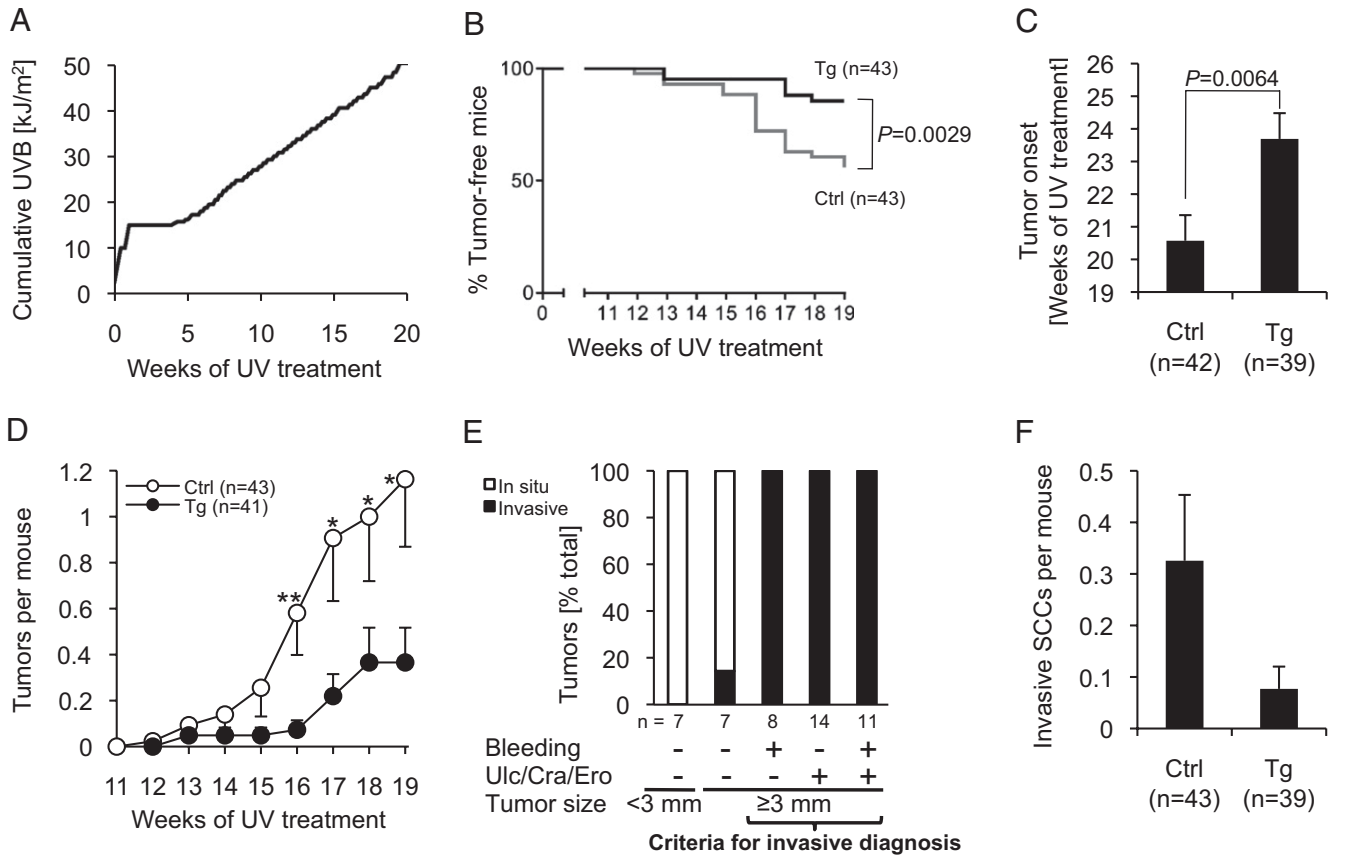

Fig. 3. ATR-kd transgene delays tumor onset and suppresses UV tumorigenesis. (*A*) UV irradiation timeline indicating cumulative UVB dosage. Mice were irradiated with 250–2,500 J/m^2 of UVB light per day, thrice weekly. (*B*) Percentage of tumor-free mice is shown for each group: ATR-kd transgenic (Tg) mice or transgene-negative littermate controls (Ctrl). All mice in both groups were *Xpc*$^{-/-}$. Kaplan–Meier curves were compared by using the logrank test for statistical significance. (*C*) Tumor onset is delayed in ATR-kd transgenic mice. Mean number of weeks of UV treatment required for developing an initial tumor is shown. (Error bars = SEM.) (*D*) ATR-kd transgene suppresses UV-induced tumor development. Mean number of tumors per mouse is shown up to 19 wk, the point when some mice with advanced tumors were killed and the cohort was no longer complete. (Error bars = SEM.) Statistical significance in mean number of tumors per mouse between the groups was as shown at the indicated time points: $*P \leq 0.05$, $**P < 0.01$. (*E*) Correlation of visible tumor features with histological tumor invasiveness in a randomly selected subset of tumors at time of euthanasia. Before histologic examination, 47 tumors (22 from ATR-kd transgenic mice and 25 from transgene-negative littermate controls) were segregated into five groups as shown based on size, bleeding, and ulceration/cratering/erosion. Larger tumors (≥3 mm) with bleeding and/or ulceration/cratering/erosion were presumed to be invasive SCCs. Indeed, all 34 tumors that had visible features associated with invasive SCCs were verified pathologically to be invasive SCCs. The 14 tumors that did not meet clinical criteria for invasive SCC were found microscopically to be SCC in situ ($n = 7$), keratoacanthoma ($n = 5$), epidermal hyperplasia ($n = 1$), and invasive SCC ($n = 1$). (*F*) ATR-kd transgenic mice had fourfold fewer clinically defined invasive SCCs than transgene-negative littermate controls (Ctrl) did, although this result did not meet statistical significance ($P = 0.071$). Mean number of invasive SCCs per mouse after 23 wk of UV treatment is shown. (Error bars = SEM.)

statistical power was not sufficient to reach significance between the two groups ($P = 0.071$). We also measured latency from initial tumor development to clinically defined invasive SCC. Among all tumors that ultimately progressed to clinically defined invasive SCCs ($n = 142$ with 68 in transgenic mice and 74 in transgene-negative littermate controls), the average latency from initial tumor detection to invasive SCC development was 22.2 ± 1.8 d (mean ± SEM). The latency in transgenic mice (18.5 ± 2.3 d, $n = 68$) was somewhat shorter than that in the transgene-negative littermate controls (25.6 ± 2.8 d, $n = 74$), a difference that approached statistical significance ($P = 0.052$).

Discussion

To investigate the effect of ATR inhibition on UV-induced skin carcinogenesis, we created a mouse model in which ATR is partially inhibited in skin. In analogy to other DNA damage response checkpoint proteins, ATR inhibition might be expected to increase genomic instability, promoting tumorigenesis. Instead, we found that ATR-kd transgenic mice were protected from UV carcinogenesis. Presence of the ATR-kd transgene mimicked the effects of caffeine and promoted apoptosis of DNA-damaged keratinocytes shortly after UV exposure. This study suggests that caffeine's UV protective effect, documented in previous human epidemiologic and mouse in vivo studies, is likely attributable to ATR inhibition. This plausible mechanism could be further validated by examining whether caffeine demonstrates an additive effect on skin cancer prevention in ATR-kd mice. Although this experiment cannot be performed in vivo because of cost, it appears that caffeine administration to ATR-kd transgenic mice would be unlikely to show further protection from UV-induced skin tumors because there was no additive effect of caffeine on UV-induced apoptosis in transgenic keratinocyte experiments (Fig. 2*D*).

Previous studies have shown that the DNA damage response is an important anticancer barrier in early tumorigenesis to cope with aberrant oncogenic stimuli and to maintain genomic integrity (31, 32). Typically, inhibiting oncogene-induced DNA damage responses via the ATM–Chk2 pathway facilitates tumor development (33–35). Furthermore, caffeine administration or ATR suppression promotes oncogenic Ras-induced tumorigenesis (33, 36). However, in the present study, we found that ATR

inhibition provided protection from UV tumorigenesis. Ras mutations are rare in UV-induced mouse skin tumors (37). What might explain the contrasting effects of ATR inhibition on Ras-induced tumorigenesis compared with UV-induced tumorigenesis? One plausible explanation is that ATR inhibition preferentially works at a precancerous stage to eliminate UV DNA-damaged cells through augmentation of apoptosis (possibly before oncogenes are activated, conferring survival advantage), preventing subsequent progression to UV-induced skin cancers. In contrast, after oncogenes have already been activated and cells suffer hyperreplicative stress, as in Ras-induced tumorigenesis, inhibition of DNA damage responses such as the ATM/ATR pathways may more likely promote genomic instability and hence tumorigenesis.

Chronic UV exposure eventually led to tumors in mice with diminished ATR function in skin, although tumor onset was significantly delayed in transgenic compared with littermate control mice. In contrast, the time required to progress from an initial tumor to an invasive SCC tended to be shorter in transgenic mice than that in littermate control mice. These findings suggest that ATR suppression diminished the early stages of UV carcinogenesis but not the progression from initial tumor to invasive SCC. Once keratinocytes acquire genetic mutations required for tumor cell survival and development, continued ATR suppression may no longer be effective in decreasing tumor development. Another possibility is that transgene expression was reduced in established tumors, explaining the lack of an effect on the rate of progression to aggressive tumors.

For prevention of UV-induced SCCs, p53-mutant keratinocytes are important targets because UV frequently induces p53 mutations in epidermal keratinocytes and SCCs often originate from p53-mutant keratinocytes (38). ATR inhibition can selectively sensitize G_1 checkpoint-deficient cells to UV (16). Also, ATR knockdown in adult mice showed synthetic lethality with p53 deficiency, suggesting that ATR inhibition may selectively eradicate p53-deficient cells (39). Indeed, topical application of caffeine on mouse skin augmented UV-induced apoptotic sunburn cells not only in $p53^{+/+}$ but also in $p53^{-/-}$ mice (40). Thus, it appears that ATR inhibition sensitizes any DNA-damaged cell type to death but that p53-mutant cells are especially susceptible to ATR inhibition.

We carried out a preliminary experiment to detect sunburn cells in ATR-kd mice (in the FVB genetic background with wild-type XPC function) treated with a single dose (30 mJ/cm^2) of UVB light. This study did not reveal differences between transgenic mice and transgene-negative littermate controls, whereas keratinocyte experiments in the present study show that ATR-kd augments UV-induced apoptosis. Our previous studies also demonstrated that caffeine (possibly via ATR inhibition) augments UV-induced apoptosis in vivo (as well as in vitro) (9, 10). One explanation for these differing results is that experimental conditions, such as UV dose and the timing of sunburn cell detection after UV exposure, might have been suboptimal. Rates of formation of sunburn cells depend on UV dose, timing after UV exposure, and genetic background (40). In hairless $Xpc^{-/-}$ mice, apoptotic cells (caspase 3-positive) were observed 24 h after 200 mJ/cm^2 of UVB light (41). Another possibility is that the expression level of ATR-kd transgene under the K14 promoter was extremely low in vivo, leading to a very small effect of ATR-kd on an acute experiment, such as sunburn cell detection after a single dose of UV. However, ATR-kd could have an effect on a cumulative basis, such as in carcinogenesis.

Outside of the observed preventive effect of ATR suppression on UV tumorigenesis, the ATR-kd transgenic mice showed no survival disadvantage, skin abnormalities, or spontaneous tumor development without UV treatment. These observations of tissue-specific inhibition of ATR function differ from previous studies of humans and mice with diminished ATR function. A splicing mutation in the *ATR* gene, causing reduced expression of ATR, is linked to human patients with Seckel syndrome characterized by bird-headed dwarfism (26). ATR hypomorphic mice with Seckel mutation showed accelerated aging and died within 6 mo after birth (21). Conditional ATR knockdown in adult mice also showed accelerated aging (42). Our results suggest that low-level, tissue-specific inhibition of the replication checkpoint is well tolerated.

SKH-1 hairless mice have been widely used as an animal model for skin cancer development because these mice are highly susceptible to UV and develop papillomas, keratoacanthomas, and SCCs after chronic UV irradiation (43, 44). Shaving wild-type haired mice does not make them as susceptible to UV as SKH-1 mice are (37), and the mechanisms of susceptibility of SKH-1 mice to UV are not well understood. Indeed, in humans, a missense mutation in the *hairless* gene is associated with complete hair loss but is not linked to UV susceptibility (45), suggesting species-specific differences in the roles for this protein. For the present study, we selected a well-characterized UV-susceptible model, $Xpc^{-/-}$ mice, that develop keratoacanthomas and SCCs after chronic UV irradiation because of DNA-repair deficiency (29). Unlike other DNA-repair deficiency models ($Xpa^{-/-}$ and $Csb^{-/-}$) in which UV-induced apoptosis is markedly augmented, $Xpc^{-/-}$ mice demonstrate similar rates of UV-induced apoptosis compared with wild-type mice (41), making this model appropriate for investigating effects of ATR inhibition on augmentation of UV-induced apoptosis. Although xeroderma pigmentosum is a rare genetic disease, XPC protein expression is lost in up to 59% of invasive SCCs from non-XPC patients (46), further increasing the relevance of this model to human skin cancer studies. Beyond the persistence of a larger amount of DNA damage after UV exposure in XPC-deficient versus wild-type cells, the subsequent progression to malignancy is not thought to differ between XPC-deficient and wild-type cells.

Although inhibiting ATM/ATR pathways promotes tumorigenesis in other settings, our findings from ATR-kd transgenic mice suggest that ATR inhibition in skin is well tolerated and suppresses UV-induced tumor development. Combined with the extensive epidemiologic data linking caffeine intake with decreased skin cancer development, these findings suggest the possibility that topical caffeine application could be useful in preventing UV-induced skin cancers. An additional appealing aspect of topical application of caffeine is that it directly absorbs UV and thus also acts as a sunscreen, potentiating the efficacy of topical UV protection (47). This chemopreventive approach via ATR inhibition might be especially beneficial for individuals at high risk of UV-associated nonmelanoma skin cancers.

Materials and Methods

Generation of ATR-kd Transgenic Mice. Amino-terminal FLAG epitope-tagged full-length construct of human ATR-kd was generated as previously described (16, 24). The construct was subcloned into the human K14 promoter construct containing an intron from the β-globin gene (23). The full expression cassette of K14–ATR-kd was then digested away from plasmid DNA sequences before injection into mouse blastocysts.

ATR-kd transgenic mice were generated at the Brigham and Women's Hospital Transgenic Mouse Core Facility with the FVB mouse strain. Presence of the ATR-kd transgene was confirmed by PCR using genomic DNA extracted from mouse tails and primers that amplified the human K14 promoter (only present in transgenic mice). A section of mouse bone morphogenic protein receptor type II (*Bmpr2*) was used as control for DNA quality in PCR experiments.

ATR-kd transgenic mice in an FVB genetic background were crossed with $Xpc^{-/-}$ mice in a mixed genetic background that contained both C57BL/6 and 129S7 (B6;129S7-*Xpc*^{tm1Brd}, model no. 000557; Taconic). The offspring were intercrossed to maintain colonies and obtain ATR-kd transgenic mice and transgene-negative littermate controls. All mice used in this study were $Xpc^{-/-}$ mice with or without the ATR-kd transgene. $Xpc^{-/-}$ genotype was confirmed by PCR to demonstrate no amplification at two loci: *Xpc* exon 3 and exon 4.

PCR for genotyping and real-time RT-PCR for detecting ATR-kd transgene expression are described in *SI Materials and Methods*.

Chronic UV Irradiation of Mice. All animal procedures were approved by the Institutional Animal Care and Use Committee at the University of Washington. Before chronic UV treatment, 11- to 44-wk-old ATR-kd transgenic mice ($n = 43$) and their transgene-negative littermate controls ($n = 43$) were selected from among larger populations so that the final groups were closely matched for age, sex, and coat color. During chronic UV treatment, mice were shaved once per week. Mice were irradiated with UVB light from FS40T12/UVB bulbs (National Biological Corporation) with peak emission between 300 and 315 nm and rapid decrease in emission beyond the UVB range (UV below 280 nm was undetectable). UVB dose was measured with a Photolight IL1400A radiometer equipped with a SEL240/UVB detector (International Light Technologies). Mice were treated with 250–2,500 J/m^2 of UVB light per day, typically thrice weekly. UV treatment was temporarily decreased or held if >20% of mice developed significant skin erythema. UV treatment continued until all mice developed at least one tumor, with the final cumulative dose of UVB light at the end of the experiment (282 d) being 166.8 kJ/m^2. Mice were monitored weekly for the development of tumors on ears and back skin. A discrete, palpable, and persistent papule was recorded as an initial tumor. An invasive SCC was defined as a larger tumor (≥3-mm tumor diameter) with evidence of bleeding and/or ulceration/cratering/erosion. Mice were euthanized if they had any of the following: a tumor ≥1 cm in diameter, persistent bleeding of any tumor, or cachexia. A description of histological analyses of tumors is provided in *SI Materials and Methods*.

Statistical Analyses. Statistical significance in mean between two groups was determined by a two-tailed, two-sample *t* test. Error bars in figures indicate SEM. Kaplan–Meier curves (Fig. 3*B*) were compared by using the logrank test for statistical significance (Prism 5; GraphPad Software). A detailed description of mice excluded from the tumor analyses shown in Fig. 3 *C*, *D*, and *F* (because of deaths unrelated to skin tumors) is included in *SI Materials and Methods*.

Isolation of Primary Keratinocytes from Transgenic Mice. Primary mouse keratinocytes were isolated from the epidermis of 1- to 3-d-old transgenic mice and transgene-negative littermate controls, as previously described (48). Detailed methods for experiments using isolated primary keratinocytes are provided in *SI Materials and Methods*.

ACKNOWLEDGMENTS. We thank Dr. Elaine Fuchs for providing the human β-globin intron-containing keratin-14 promoter construct. This work was supported by National Institutes of Health Grants R01-AR049832 (to P.N.) and R01-CA130857 (to A.H.C.).

1. Jacobsen BK, Bjelke E, Kvåle G, Heuch I (1986) Coffee drinking, mortality, and cancer incidence: Results from a Norwegian prospective study. *J Natl Cancer Inst* 76:823–831.
2. Hakim IA, Harris RB, Weisgerber UM (2000) Tea intake and squamous cell carcinoma of the skin: Influence of type of tea beverages. *Cancer Epidemiol Biomarkers Prev* 9: 727–731.
3. Abel EL, et al. (2007) Daily coffee consumption and prevalence of nonmelanoma skin cancer in Caucasian women. *Eur J Cancer Prev* 16:446–452.
4. Rees JR, et al. (2007) Tea consumption and basal cell and squamous cell skin cancer: Results of a case-control study. *J Am Acad Dermatol* 56:781–785.
5. Arab L (2010) Epidemiologic evidence on coffee and cancer. *Nutr Cancer* 62:271–283.
6. Huang MT, et al. (1997) Effects of tea, decaffeinated tea, and caffeine on UVB light-induced complete carcinogenesis in SKH-1 mice: Demonstration of caffeine as a biologically important constituent of tea. *Cancer Res* 57:2623–2629.
7. Lu YP, et al. (2002) Topical applications of caffeine or (–)-epigallocatechin gallate (EGCG) inhibit carcinogenesis and selectively increase apoptosis in UVB-induced skin tumors in mice. *Proc Natl Acad Sci USA* 99:12455–12460.
8. Zhang W, et al. (2005) UVB-induced apoptosis drives clonal expansion during skin tumor development. *Carcinogenesis* 26:249–257.
9. Lu YP, et al. (2002) Stimulatory effect of topical application of caffeine on UVB-induced apoptosis in mouse skin. *Oncol Res* 13:61–70.
10. Koo SW, Hirakawa S, Fujii S, Kawasumi M, Nghiem P (2007) Protection from photodamage by topical application of caffeine after ultraviolet irradiation. *Br J Dermatol* 156:957–964.
11. Sarkaria JN, et al. (1999) Inhibition of ATM and ATR kinase activities by the radiosensitizing agent, caffeine. *Cancer Res* 59:4375–4382.
12. Zhou BB, Bartek J (2004) Targeting the checkpoint kinases: Chemosensitization versus chemoprotection. *Nat Rev Cancer* 4:216–225.
13. Lapenna S, Giordano A (2009) Cell cycle kinases as therapeutic targets for cancer. *Nat Rev Drug Discov* 8:547–566.
14. Sabisz M, Skladanowski A (2008) Modulation of cellular response to anticancer treatment by caffeine: Inhibition of cell cycle checkpoints, DNA repair and more. *Curr Pharm Biotechnol* 9:325–336.
15. Foukas LC, et al. (2002) Direct effects of caffeine and theophylline on p110 delta and other phosphoinositide 3-kinases. Differential effects on lipid kinase and protein kinase activities. *J Biol Chem* 277:37124–37130.
16. Nghiem P, Park PK, Kim Y, Vaziri C, Schreiber SL (2001) ATR inhibition selectively sensitizes G_1 checkpoint-deficient cells to lethal premature chromatin condensation. *Proc Natl Acad Sci USA* 98:9092–9097.
17. Bucher N, Britten CD (2008) G2 checkpoint abrogation and checkpoint kinase-1 targeting in the treatment of cancer. *Br J Cancer* 98:523–528.
18. Li S, et al. (2000) Functional link of BRCA1 and ataxia telangiectasia gene product in DNA damage response. *Nature* 406:210–215.
19. Khanna KK, Jackson SP (2001) DNA double-strand breaks: Signaling, repair and the cancer connection. *Nat Genet* 27:247–254.
20. Brown EJ, Baltimore D (2000) ATR disruption leads to chromosomal fragmentation and early embryonic lethality. *Genes Dev* 14:397–402.
21. Murga M, et al. (2009) A mouse model of ATR-Seckel shows embryonic replicative stress and accelerated aging. *Nat Genet* 41:891–898.
22. Vassar R, Rosenberg M, Ross S, Tyner A, Fuchs E (1989) Tissue-specific and differentiation-specific expression of a human K14 keratin gene in transgenic mice. *Proc Natl Acad Sci USA* 86:1563–1567.
23. Vasioukhin V, Degenstein L, Wise B, Fuchs E (1999) The magical touch: Genome targeting in epidermal stem cells induced by tamoxifen application to mouse skin. *Proc Natl Acad Sci USA* 96:8551–8556.
24. Cliby WA, et al. (1998) Overexpression of a kinase-inactive ATR protein causes sensitivity to DNA-damaging agents and defects in cell cycle checkpoints. *EMBO J* 17: 159–169.
25. Wang J, et al. (2004) ATM-dependent CHK2 activation induced by anticancer agent, irofulven. *J Biol Chem* 279:39584–39592.
26. O'Driscoll M, Ruiz-Perez VL, Woods CG, Jeggo PA, Goodship JA (2003) A splicing mutation affecting expression of ataxia-telangiectasia and Rad3-related protein (ATR) results in Seckel syndrome. *Nat Genet* 33:497–501.
27. Wilsker D, Bunz F (2007) Loss of ataxia telangiectasia mutated- and Rad3-related function potentiates the effects of chemotherapeutic drugs on cancer cell survival. *Mol Cancer Ther* 6:1406–1413.
28. Heffernan TP, et al. (2009) ATR–Chk1 pathway inhibition promotes apoptosis after UV treatment in primary human keratinocytes: Potential basis for the UV protective effects of caffeine. *J Invest Dermatol* 129:1805–1815.
29. Sands AT, Abuin A, Sanchez A, Conti CJ, Bradley A (1995) High susceptibility to ultraviolet-induced carcinogenesis in mice lacking XPC. *Nature* 377:162–165.
30. Bakkenist CJ, Kastan MB (2003) DNA damage activates ATM through intermolecular autophosphorylation and dimer dissociation. *Nature* 421:499–506.
31. Bartkova J, et al. (2005) DNA damage response as a candidate anti-cancer barrier in early human tumorigenesis. *Nature* 434:864–870.
32. Gorgoulis VG, et al. (2005) Activation of the DNA damage checkpoint and genomic instability in human precancerous lesions. *Nature* 434:907–913.
33. Bartkova J, et al. (2006) Oncogene-induced senescence is part of the tumorigenesis barrier imposed by DNA damage checkpoints. *Nature* 444:633–637.
34. Di Micco R, et al. (2006) Oncogene-induced senescence is a DNA damage response triggered by DNA hyper-replication. *Nature* 444:638–642.
35. Pusapati RV, et al. (2006) ATM promotes apoptosis and suppresses tumorigenesis in response to Myc. *Proc Natl Acad Sci USA* 103:1446–1451.
36. Gilad O, et al. (2010) Combining ATR suppression with oncogenic Ras synergistically increases genomic instability, causing synthetic lethality or tumorigenesis in a dosage-dependent manner. *Cancer Res* 70:9693–9702.
37. Khan SG, et al. (1996) Mutations in ras oncogenes: Rare events in ultraviolet B radiation-induced mouse skin tumorigenesis. *Mol Carcinog* 15:96–103.
38. Ziegler A, et al. (1994) Sunburn and p53 in the onset of skin cancer. *Nature* 372: 773–776.
39. Ruzankina Y, et al. (2009) Tissue regenerative delays and synthetic lethality in adult mice after combined deletion of Atr and Trp53. *Nat Genet* 41:1144–1149.
40. Lu YP, Lou YR, Peng QY, Xie JG, Conney AH (2004) Stimulatory effect of topical application of caffeine on UVB-induced apoptosis in the epidermis of p53 and Bax knockout mice. *Cancer Res* 64:5020–5027.
41. van Oosten M, et al. (2000) Differential role of transcription-coupled repair in UVB-induced G_2 arrest and apoptosis in mouse epidermis. *Proc Natl Acad Sci USA* 97: 11268–11273.
42. Ruzankina Y, et al. (2007) Deletion of the developmentally essential gene ATR in adult mice leads to age-related phenotypes and stem cell loss. *Cell Stem Cell* 1: 113–126.
43. Gallagher CH, Canfield PJ, Greenoak GE, Reeve VE (1984) Characterization and histogenesis of tumors in the hairless mouse produced by low-dosage incremental ultraviolet radiation. *J Invest Dermatol* 83:169–174.
44. Benavides F, Oberyszyn TM, VanBuskirk AM, Reeve VE, Kusewitt DF (2009) The hairless mouse in skin research. *J Dermatol Sci* 53:10–18.
45. Ahmad W, et al. (1998) Alopecia universalis associated with a mutation in the human *hairless* gene. *Science* 279:720–724.
46. de Feraudy S, et al. (2010) The DNA damage-binding protein XPC is a frequent target for inactivation in squamous cell carcinomas. *Am J Pathol* 177:555–562.
47. Lu YP, et al. (2007) Caffeine and caffeine sodium benzoate have a sunscreen effect, enhance UVB-induced apoptosis, and inhibit UVB-induced skin carcinogenesis in SKH-1 mice. *Carcinogenesis* 28:199–206.
48. Lichti U, Anders J, Yuspa SH (2008) Isolation and short-term culture of primary keratinocytes, hair follicle populations and dermal cells from newborn mice and keratinocytes from adult mice for in vitro analysis and for grafting to immunodeficient mice. *Nat Protoc* 3:799–810.

Supporting Information

Kawasumi et al. 10.1073/pnas.1111378108

SI Materials and Methods

PCR for Genotyping. PCR primers for the human keratin-14 (K14) promoter [only present in ATR-kd transgenic mice, which are mice that express a kinase-dead form of human ataxia telangiectasia and Rad3-related (ATR)] were: forward, 5′-CACGATACACCTGACTAGCTGGCTG-3′ and reverse, 5′-CATCACCCACAGGCTAGCCCCAACT-3′. PCR primers for mouse bone morphogenic protein receptor type II (*Bmpr2*) were: forward, 5′-CACACCAGCCTTATACTCTAGATA-3′ and reverse, 5′-CACATATCTGTTATGAAACTTGAG-3′. PCR primers for mouse *Xpc* exon 3 were: forward, 5′-GAACGGGAAAGAAGGTAGGC-3′ and reverse, 5′-GGTCCTCCACTCACTGGCTA-3′. PCR primers for mouse *Xpc* exon 4 were: forward, 5′-TTTGCCATTTTCCCATGAGT-3′ and reverse, 5′-TCGTGATCCTACCAGCCTTC-3′. Thermal cycling conditions for PCR amplification of ATR-kd transgene, *Bmpr2*, and *Xpc* were 94 °C for 3 min; [94 °C for 1 min, 60 °C for 2 min, 72 °C for 1 min] × 35 cycles; and 72 °C for 10 min.

Real-Time RT-PCR for Detecting ATR-kd Transgene Expression. RNA was isolated from mouse tail snips with TRI Reagent (Sigma-Aldrich) according to the manufacturer's instructions. Real-time RT-PCR was carried out in a one-step process with TaqMan EZ RT-PCR Core Reagents (Applied Biosystems) or a two-step process with High-Capacity cDNA Reverse Transcription Kit (Applied Biosystems) and TaqMan Universal PCR Master Mix (Applied Biosystems). The Applied Biosystems 7900 HT or 7700 Sequence Detection Systems were used for real-time PCR and one-step real-time RT-PCR. The Eppendorf Mastercycler was used for the reverse transcription step of the two-step protocol. Primers for amplification of ATR-kd transgene were as follows: forward, 5′-CTATAAAGATGACGATGACAAGGGTG-3′ and reverse, 5′-TGTGGCACTGCCCAGCT-3′. Probe for quantification of ATR-kd transgene amplicons was 5′-6-FAM-CTGGCTTCCATGATCCCCGCC-BHQ-1-3′. Primers for amplification of the mouse *Gapdh* gene were: forward, 5′-TCACTGGCATGGCCTTCC-3′ and reverse, 5′-GGCGGCACGTCAGATCC-3′. Probe for quantification of *Gapdh* amplicons was 5′-JOE-TTCCTACCCCCAATGTGTCCGTCG-BHQ-1-3′. Thermal cycling condition for one-step real-time RT-PCR was 50 °C for 2 min; 95 °C for 10 min; and [95 °C for 15 s, 60 °C for 1 min] × 40 cycles.

Histological Analyses of Tumors. Skin specimens containing tumors were excised from back skin and ears of chronically UV-irradiated mice at time of euthanasia. Skin was placed onto a rigid sheet of plastic with a filter paper and fixed in 10% phosphate-buffered formalin for 24 h, followed by prolonged storage in 70% ethanol. Skin specimens were paraffin-embedded, sectioned, and stained with hematoxylin and eosin. Histological diagnoses were made by experienced veterinary pathologists. A key feature of tumor invasiveness was penetration of dysplastic tumor cells through the basement membrane into the dermis.

UV Irradiation of Primary Keratinocytes. Primary keratinocytes isolated from transgenic mice and transgene-negative littermate controls were cultured in PCT Epidermal Keratinocyte Medium (CnT-07; CELLnTEC Advanced Cell Systems) supplemented with Antibiotic/Antimycotic Solution (CnT-ABM; CELLnTEC Advanced Cell Systems) on dishes coated with collagen I (Inamed) and maintained at 37 °C in a humidified atmosphere of 5% CO_2. Experiments were conducted on logarithmically growing primary keratinocytes without passaging.

Caffeine (Sigma-Aldrich) was dissolved in Dulbecco's PBS (Invitrogen) to a final concentration of 100 mM. Keratinocyte medium with or without 3 mM caffeine was prepared. Then, cultured medium was replaced with the caffeine-containing medium at 30 min before UVB treatment. Immediately before UVB treatment, culture medium containing caffeine was removed and reserved. Cells were rinsed once with warm PBS and irradiated with 75 mJ/cm^2 of UVB light by a panel of four UVB bulbs (RPR-3000; Southern New England UV), emitting radiation centered around 311 nm, covered with a Kodacel filter (K6808; Eastman Kodak) to eliminate any UVC light. UVB dose was monitored with a Photolight IL1400A radiometer. After irradiation, the reserved medium was replaced, and cells were incubated at 37 °C in a humidified atmosphere of 5% CO_2 for 1 h for immunoblot analyses or 24 h for flow cytometry analysis. Sham-treated cells were handled exactly the same way, except that they were not exposed to UVB light.

Flow Cytometry Analysis for Sub-2N DNA Content. For measuring sub-2N DNA content, cells were trypsinized and harvested 24 h after UVB irradiation. Cells were fixed with 70% ethanol for 1 h at 4 °C. Cells were washed once with PBS, treated with 1 mg/mL ribonuclease A (Sigma-Aldrich) for 30 min at 37 °C, and stained with 50 μg/mL propidium iodide (Sigma-Aldrich). Cells were analyzed on a Cytomics FC 500 (Beckman Coulter) flow cytometer. The acquired data were analyzed with CXP Analysis 2.2 (Beckman Coulter).

Doxorubicin Treatment to Primary Keratinocytes. Doxorubicin (EMD Biosciences) was dissolved in water to a final concentration of 10 mM. Keratinocyte medium with or without 1 μM doxorubicin was first prepared. Then, cultured medium was replaced with the doxorubicin-containing medium. Cells were incubated for 2 h at 37 °C in a humidified atmosphere of 5% CO_2.

Immunoblot Analyses. Cells were harvested by trypsinization 1 h after UV exposure or 2 h after doxorubicin treatment. Cell suspensions were collected in 1.7-mL tubes and centrifuged at 450 × *g* for 10 min at 4 °C. Cell pellets were washed once in PBS and centrifuged again at 450 × *g* for 10 min at 4 °C. Cell pellets were resuspended in cell lysis buffer (Cell Signaling Technology) supplemented with Complete Protease Inhibitor Cocktail (Roche Applied Science) and PhosSTOP Phosphatase Inhibitor Cocktail (Roche Applied Science). After incubating on ice for 10 min, cell lysates were clarified by centrifugation at 22,000 × *g* for 5 min at 4 °C. Protein concentrations of cell lysates were determined by using the Bradford Protein Assay Dye Reagent (Bio-Rad Laboratories). Cell lysates containing equal amounts of total protein [10 μg for phospho-checkpoint kinase 1 (Chk1) detection and 15 μg for phospho-ataxia telangiectasia mutated (ATM) detection] were mixed with NuPAGE LDS Sample Buffer (Invitrogen) containing 2-mercaptoethanol (Sigma-Aldrich) and heated at 70 °C for 10 min. Protein samples were separated in NuPAGE 3–8% Tris-Acetate Gel (Invitrogen) with NuPAGE Tris-Acetate SDS Running Buffer (Invitrogen). Proteins were transferred to Immobilon-P PVDF Membrane (Millipore) and probed with antibodies against FLAG (M5) (F4042; Sigma-Aldrich), ATR (AHP384; AbD Serotec MorphoSys), phospho-Chk1 (Ser^{345}) (133D3, 2348; Cell Signaling Technology), phospho-ATM (Ser^{1981}) (200-301-400; Rockland Immunochemicals), ATM

(ab78; Abcam), tubulin (ab4074; Abcam), and tubulin-HRP (ab40742; Abcam). For chemiluminescent detection, HRP-conjugated anti-rabbit (NA9340) and anti-mouse (NA931) secondary antibodies (GE Healthcare) and ECL Western Blotting Detection Reagents (GE Healthcare) were used. Signals were exposed to Kodak BioMax XAR Film (Carestream Health).

Immunoprecipitation. Anti-FLAG (M2) Affinity Gel (A2220; Sigma-Aldrich) was used to immunoprecipitate FLAG-tagged proteins in cell lysates. Affinity gel was prewashed with Tris-buffered saline (10 mM Tris·HCl, pH 8.0/150 mM NaCl) and centrifuged at 8,000 × *g* for 1 min at 4 °C four times. Cell lysates of untreated primary keratinocytes were prepared as mentioned above. Cell lysate containing 500 μg of total protein was mixed with 10 μL of packed gel volume of prewashed anti-FLAG affinity gel in a final volume of 200 μL and incubated at 4 °C overnight by rotating. Affinity gel was washed with Tris-buffered saline and centrifuged at 8,000 × *g* for 1 min at 4 °C three times. Affinity gel was mixed with NuPAGE LDS Sample Buffer (Invitrogen) containing 2-mercaptoethanol (Sigma-Aldrich) and heated at 70 °C for 10 min. After brief centrifugation, supernatant of immunoprecipitated sample was loaded and separated in NuPAGE 3–8% Tris-Acetate Gel (Invitrogen) with NuPAGE Tris-Acetate SDS Running Buffer (Invitrogen), followed by immunoblot analyses.

Data Exclusion from Tumor Analyses. Two mice were excluded from tumor analyses (Fig. 3 *C*, *D*, and *F*) because one ATR-kd transgenic mouse died spontaneously before tumor development, and one transgenic mouse was euthanized before tumor development because of cachexia. Three other mice were excluded from tumor onset analysis (Fig. 3*C*) because one transgene-negative littermate control mouse was euthanized before tumor development because of cachexia, one transgenic mouse died spontaneously before tumor development, and one transgenic mouse was euthanized before tumor development because of eye bleeding. Two more transgenic mice were excluded from invasive squamous cell carcinoma (SCC) analysis (Fig. 3*F*) because the mice died spontaneously before the time point of the analysis (23 wk of UV treatment).